# Supporting Information for

## "Surface plasmon polariton triggered Z-scheme for overall water splitting and solely light induced hydrogen generation" by:

D. Zabelin[a], A. Zabelina[a], A. Tulupova[a], R. Elashnikov[a], Z. Kolska[b], V. Svorcik[a], O. Lyutakov[a]

[a] *Department of Solid State Engineering, University of Chemistry and Technology, 16628 Prague, Czech Republic*

[b] *Faculty of Science, J. E. Purkyně University, 40096 Ústí nad Labem, Czech Republic*

---

* *Corresponding author: lyutakoo@vscht.cz*

## Experimental

### Materials and samples preparation

Sodium tungstate dihydrate (≥ 99 %), tetrafluoroboric acid (48 wt. % in the water), cadmium chloride monohydrate (99.995 %), sodium sulphide nonahydrate (≥ 99.99 %) and deionized water were purchased from Sigma-Aldrich. Ethanol (p.a. 96 %) and methanol (p.a. 99.96 %) were purchased from Lachner.

***$WO_3$ nanoflakes preparation.*** Sodium tungstate dihydrate (0.5 g) was dissolved in 25 ml of deionized water under magnetic stirring. During vigorous stirring, 1.5 ml of 40 % tetrafluoroboric acid was added dropwise into the solution. After stirring for ten minutes, the solution was transferred to a Teflon autoclave, which was placed in an oven and heated at 180° C for 10 hours. The resulting product was centrifuged and purified twice with deionized water twice with ethanol and then dried in oven at 60° C for 5 hours. The resulting powder was subjected to calcination at 400° C for 3 hours.

***Synthesis of CdS on $WO_3$ nanoflakes surface.*** A suspension of tungsten oxide (0.1 g) in 30 ml of deionized water was prepared using ultrasonication. 2 ml of a 0.1 M solution of cadmium chloride were added dropwise slowly to the suspension under vigorous stirring. After 30 min, 2 ml of 0.1 M sodium sulphide solution was carefully added dropwise to the solution. As a result cadmium sulphide precipitated on the surface of the tungsten oxide, since the cadmium ions were already attached to the surface of the $WO_3$ particles. The resulting water-soluble sodium chloride was removed from the product by centrifugation and by washing twice with deionized water. The substance was further dried in an oven at 60° C for 2 hours.

***Preparation of plasmon active Au grating.*** The creation of a plasmon-active periodic structure consists of following steps. First, a batch substrate was prepared from a DVD-R disc by

separating two transverse portions of the disc with methanol. Then the substrate was thoroughly washed with methanol solution and dried under vacuum and Au layer was deposited on the periodic surface by magnetron sputtering (40 mA, 300 s, thickness 30 nm)

***Deposition of $WO_3$-CdS on grating surface.*** First, the selection of the optimal regime for the deposition of the $WO_3$-CdS system on the Au grating surface was carried out. Namely, drop-casting and spin-coating deposition techniques were used and the result of the deposition was examined by Raman spectroscopy mapping. It was found that the spin coating method leads to more evenly distributed $WO_3$-CdS system over the grating surface. The optimal deposition parameters were: concentration of $WO_3$-CdS suspension 1.1 mg $mL^{-1}$, the speed rotation 250 rpm, and time of spin-coating 2 min.

**Measurement techniques**

***Materials characterization.*** X-ray photoelectron spectroscopy (XPS) was performed using an Omicron Nanotechnology ESCAProbeP spectrometer with a monochromated Al K Alpha X-ray source operating at 1486.6 eV. The energy resolution was 0.4 eV for the survey study and 0.1 eV for the high-resolution XPS spectra measurements. The concentrations of elements were calculated in at. % using the sensitivity factors provided by the manufacturer. Raman spectra were measured using ProRaman-L spectrometer (Enwave Optronics) (Laser power 90 mW) with 785 nm excitation wavelengths. Spectra were measured 30 times, each of them with 3 s accumulation time. UV-Vis absorption spectra were measured using a Lambda 25 UV/Vis/NIR Spectrometer (PerkinElmer, USA) at a scanning rate of 480 nm $min^{-1}$. X-ray diffraction microscopy spectra were recorded on a microXRD D8 Discover diffractometer for 30 min using Cu Kα radiation (1.5405 Å) 3 at 30 mA and 40 kV. Zeta potential measurement was carried out on Zetasizer Ultra (Malvern Pananalytical). HRTEM measurements were performed using an EFTEM Jeol 2200 FS microscope (Jeol, Japan). The CdS nanostructure distribution was calculated from HRTEM images that were obtained from three $WO_3$-CdS samples, prepared in three different syntheses prepared under identical conditions. SEM-EDX measurements were carried out on (LYRA3 GMU, Tescan, CR) equipment using accelerating voltages 10 and 2 kV. The AFM scans were obtained on the Icon (Bruker) microscope in Scan-Asyst mode.

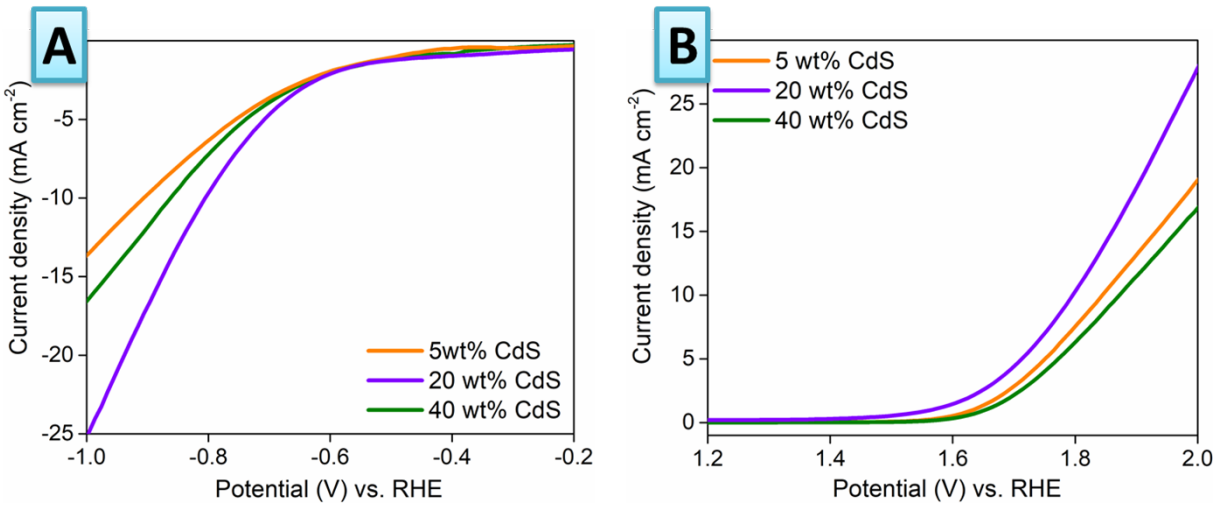


**Fig. S1** Additional LSV scans of (A) HER and (B) OER $WO_3$-CdS with different CdS concentration in 1M KOH

***Fig. S1 – description note***

The optimization of WO3 and CdS molar ratio is presented in Fig. S1. We used different $WO_3$:CdS ratio and estimate the catalytic ac6tivity by common electrochemical approach. Obtained results reveal the electrochemical activity of materials in both water splitting half-reactions. As is evident the previously reported [https://doi.org/10.1021/cs500794j] molar ratio (i.e. 20% CdS) is really optimal since it corresponds with the lower values of overpotential(s) for both, HER and OER. Thus, this ratio was further used in subsequent experiments.

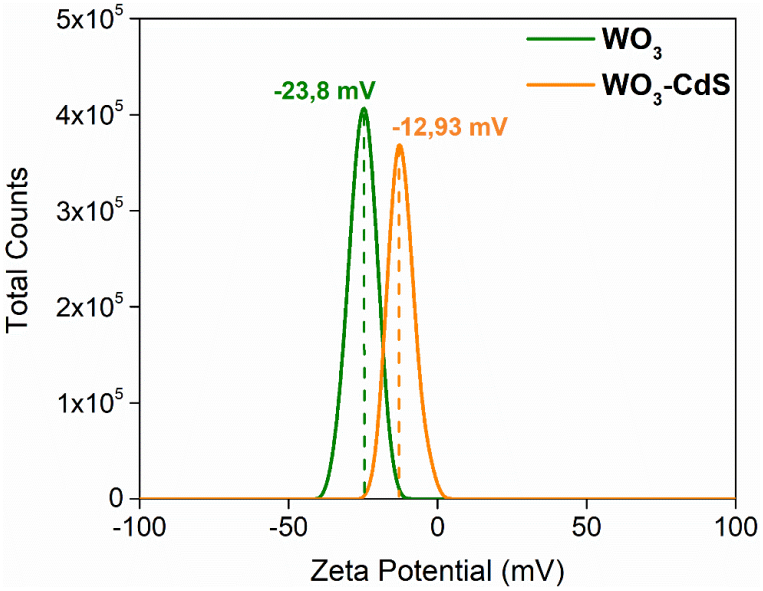


**Fig. S2** Zeta potential analysis (measurement of surface charge) of $WO_3$ flakes before and after the synthesis of CdS on flakes surface.

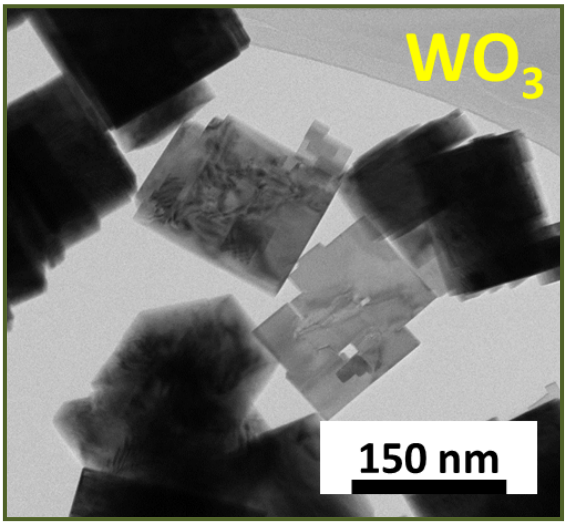


**Fig. S3** TEM image of pristine $WO_3$ flakes.

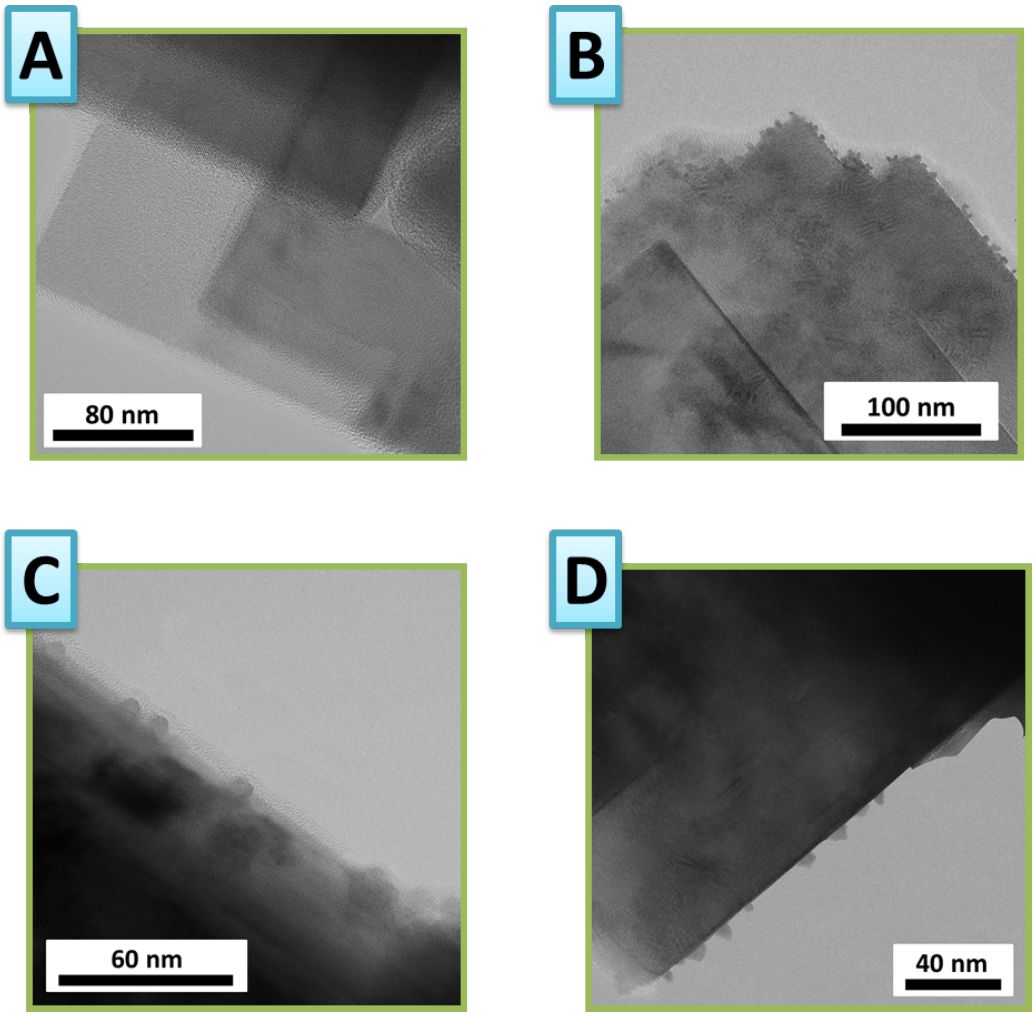


**Fig. S4** HRTEM images of (A) pristine $WO_3$ nanoflakes, (B-D) $WO_3$-CdS sample (prepared in three different syntheses).

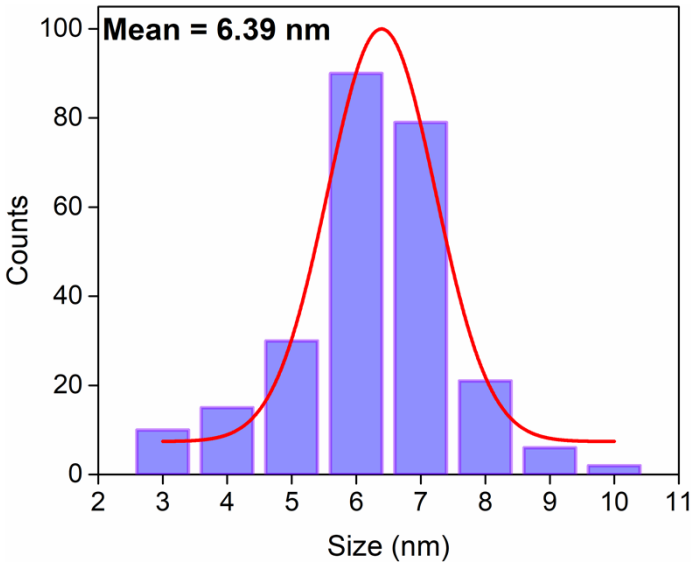


**Fig. S5** CdS size distribution, calculated from HRTEM images.

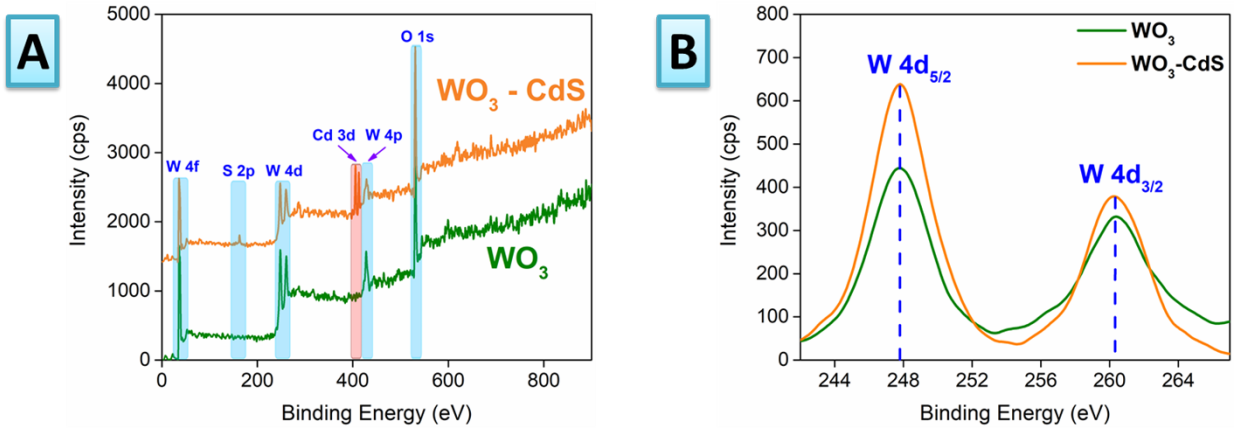


C

| | W (at.%) | O (at.%) | Cd (at.%) | S (at.%) |
|---|---|---|---|---|
| $WO_3$ | 29.39 | 70.61 | - | - |
| $WO_3$-CdS | 26.17 | 66.62 | 3.68 | 3.53 |

**Fig. S6** XPS spectra and measurements results: (A), (B) - $WO_3$ and $WO_3$-CdS flakes; (C) – surface elements concentration (in at. %) calculated from survey XPS spectra.

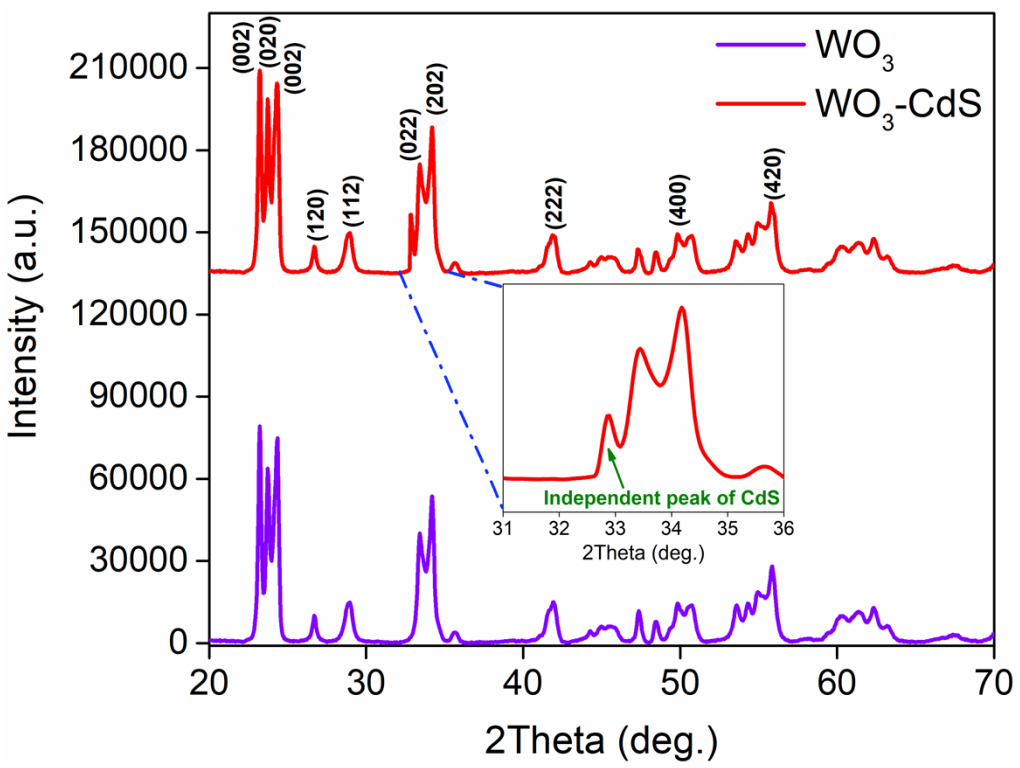


**Fig. S7** XRD pattern of $WO_3$ and $WO_3$-CdS flakes (insert shows details of the apparent splitting of characteristic W band). Peaks affiliation is given in accordance to ICSD database (monoclinic γ-$WO_3$ (ICSD #80056) and monoclinic ε-$WO_3$ (ICSD #84163)).

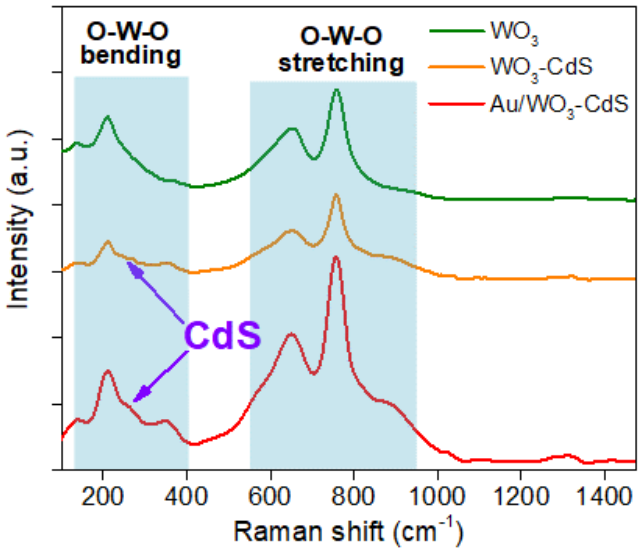


**Fig. S8** Raman spectra of $WO_3$ and $WO_3$-CdS flakes and SERS spectrum of $WO_3$-CdS flakes (after their deposition on plasmon-active Au grating surface). Peaks affiliation is given according to [S1, S2].

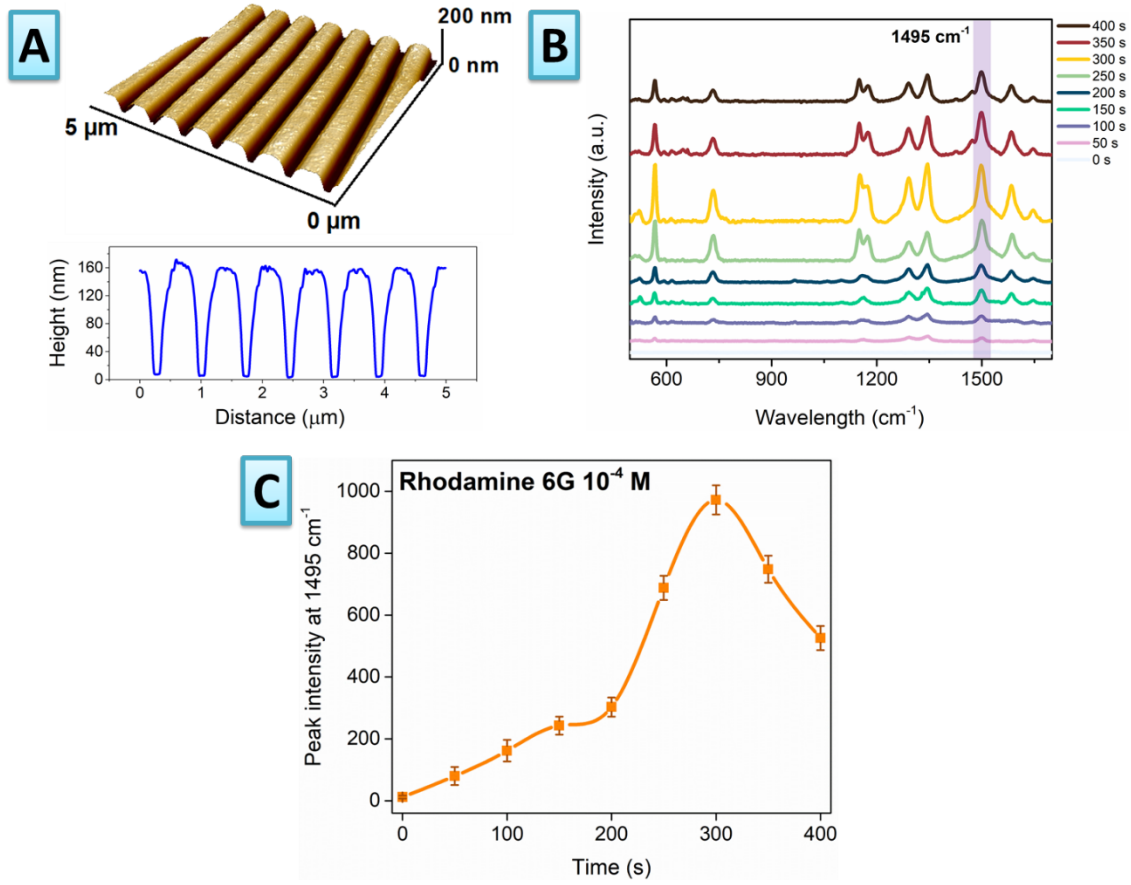


**Fig. S9** (A) – surface morphology and corresponding surface profile of pristine Au grating; (B) – optimization of grating parameters using SERS response of characteristic probe molecule (R6G)

depicted as a function of Au sputtering time; (C) - dependence of the intensity of the R6G peak (1495 $cm^{-1}$) on Au deposition time (i.e. thickness of Au layer).

***Fig. S9 – description note***

The periodical grating surface is presented in Fig. S9A. The surface regularity ensures the excitation and propagation of the so-called surface plasmon-polariton wave SPP [S3]. The efficiency of SPP excitation depends on the geometrical parameters of grating and the thickness of deposited Au layers. Since the basic geometrical parameters were determined by the morphology of the used polymer template (DVD disk), we focused our attention on the thickness of the deposited Au layers. The "strength" of SPP on the grating surface can be optimized using typical SERS probe – R6G. We deposited R6G onto grating surface and measured SERS spectra intensity as a function of Au thickness. The SERS spectra of R6G are presented in Fig. S9B. As is evident, the intensity of the SERS signal from R6G increases gradually up to the certain value of Au thickness (determined by sputtering time) and then it decreases. The characteristic R6G band was plotted as a function of Au sputtering time in Fig. S9C. As is evident, the highest value of SERS signal intensity was observed for 300s Au deposition time, corresponding to about 25 nm thick Au layer in our experimental arrangement (layer thickness was determined from AFM scratch tests performed on the control samples prepared by Au deposition on a hard substrate). So, taking into account the SERS experiments, the 300 s deposition time was used in all subsequent experiments, with the aim to ensure Z-scheme triggering by SPP as strong as possible.

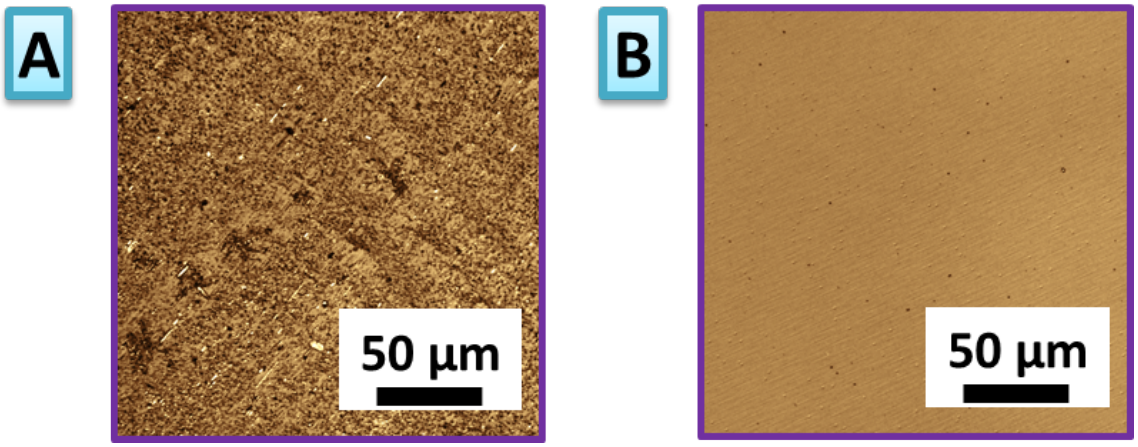


**Fig. S10** Examples of "bad" (A) and "good" (B) distribution of $WO_3$-CdS flakes on Au grating surface.

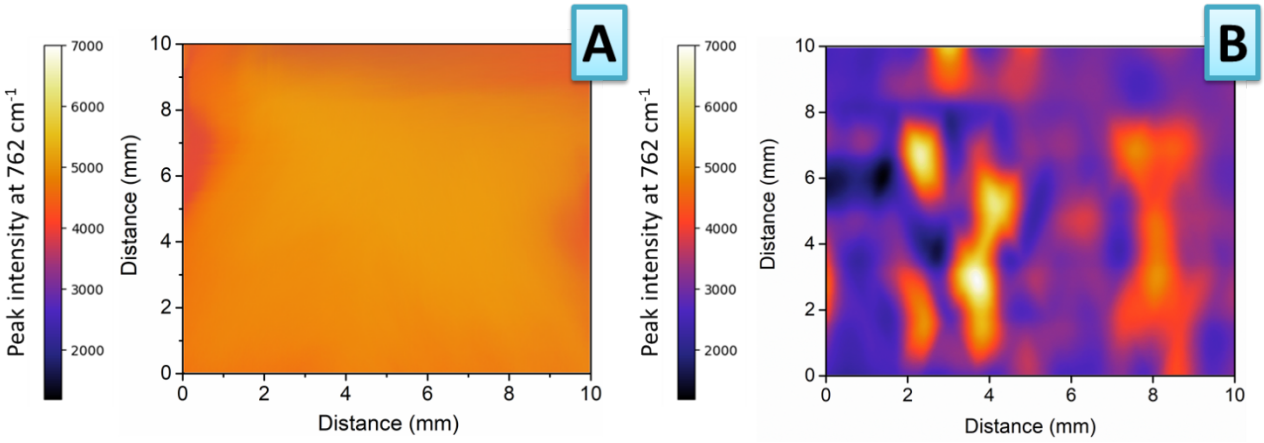


**Fig. S11** – Raman maps, measured during optimization of $WO_3$-CdS flakes deposition on Au grating surface: (A) – required homogeneous distribution of flakes (which was also conserved after reduction of the flakes layer thickness – final image is given in main manuscript text); (B) – shows result of an unsuccessful deposition in which almost all flakes were removed during spin-coating.

***Figs. S10, S11 – description note***

The deposition of $WO_3$-CdS flakes was performed using the spin-coating from methanol suspensions with various concentrations (0.2 – 5 mg $mL^{-1}$) and at different rotation speed (100 – 3000 rmp). An optimization of the deposition was performed with the aim to reach the homogeneous covering of grating surface by flakes, without the formation of flakes agglomerates. For this purpose, the homogeneity of flakes distribution was checked using optical microscopy and Raman mapping (Fig. S10 and S11). In particular, the "bad" flakes distribution (100 rpm, 5 mg $mL^{-1}$ concentration) is presented in Fig. S10A. In this case, the apparent surface roughening is well evident even in optical microscope. Such morphology can be attributed to the formation of flakes agglomerate and surface covering by a thick flakes layer. In this case, the efficient SPP triggering of "top" flakes, which are "in contact" with water cannot be expected.

In turn, Fig. S11B shows the opposite situation, where the Raman mapping reveals a non-homogeneous coverage of grating surface by flakes (3000 rmp, 0.5 mg $mL^{-1}$ concentration). The characteristic SERS bands from the flakes were observed only on a small part of the surface. In such a case, the overall structure efficiency should be close to zero, since just a small part of the Au grating is covered by redox-active material.

Finally, Figs. S10B and S11A represent a more favourable case – the microscopy image reveals the conservation of homogenous surface geometry (typical for a pristine grating), while SERS mapping indicates the homogenous signal from flakes across the overall mapped area (250 rmp. 1.5 mg $mL^{-1}$ concentration). So, in this case, the grating surface is uniformly covered by redox-active

$WO_3$-CdS flakes. In the next step, we continued with deposition experiments, by gradually decreasing flakes concentration in suspension (but with the same spin-coating speed). The concentration was reduced up to disruption of SERS signal uniformity. Optimal results achieved under 250 rpm and 1.1 mg $mL^{-1}$ flakes concentration are presented in the main manuscript text. The thickness of the flakes layer was estimated from control AFM scratch tests (performed on a hard substrate) and the known flake thickness. It was found to be in the 10-20 nm range, which corresponds to a formation of 3-5 flakes bundle.

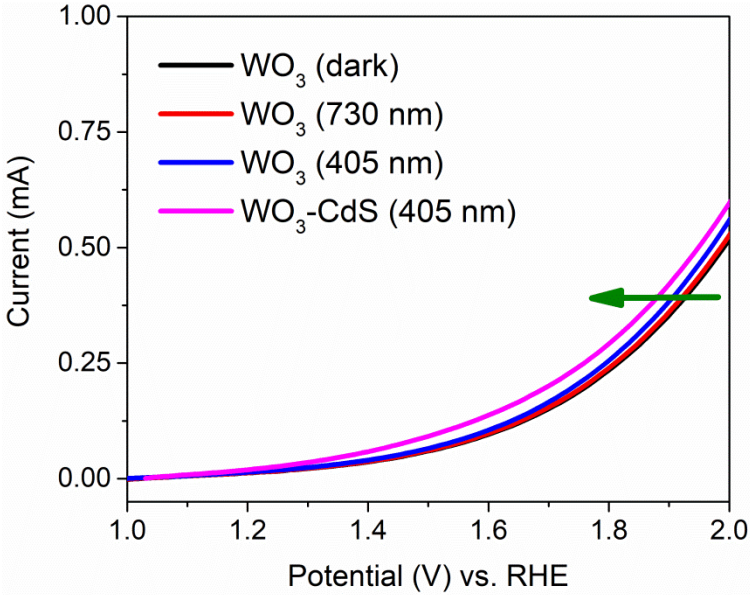


**Fig. S12** – $WO_3$ illumination control: OER half-reaction, performed on $WO_3$ flakes, deposited on non-plasmonic surface (in darkness and under illumination with 405 and 730 nm wavelengths)

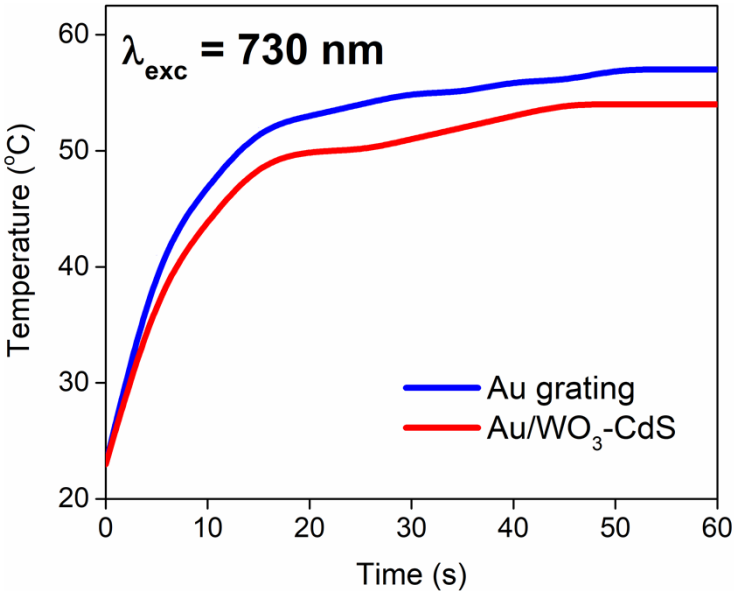


**Fig. S13** Surface temperature of Au grating and Au grating with deposited $WO_3$-CdS flakes under the continuous illumination with 730 nm LED depicted as a function of the illumination time

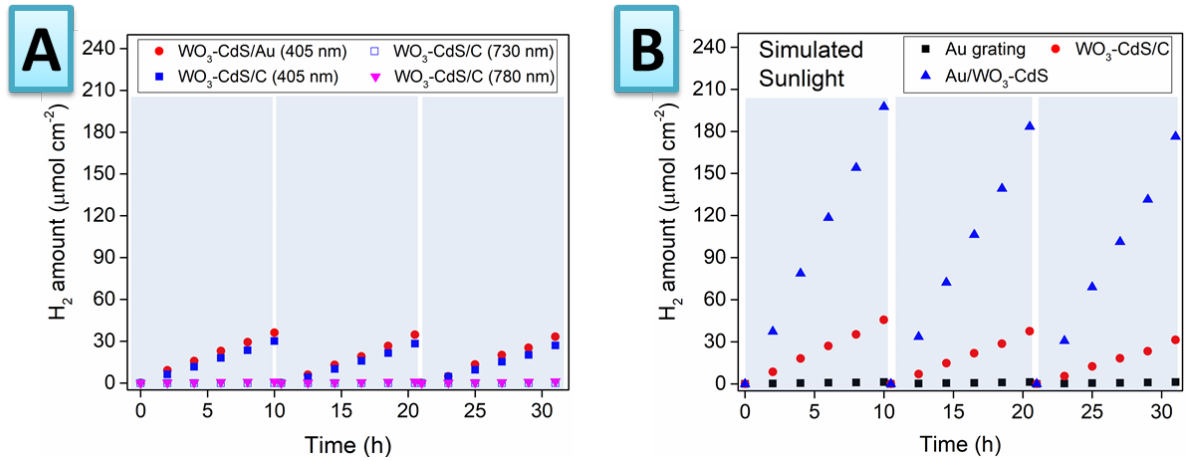


**Fig. S14** (A) – comparison of hydrogen production under illumination with simulated sunlight of Au grating, $WO_3$-CdS flakes (deposited on non-plasmonic substrate - carbon surface, designated as $WO_3$-CdS/C) and on $WO_3$-CdS/Au samples; (B) – comparison of hydrogen production under 405 or 730 nm LED illumination of $WO_3$-CdS flakes deposited on Au grating or non-plasmonic surface.

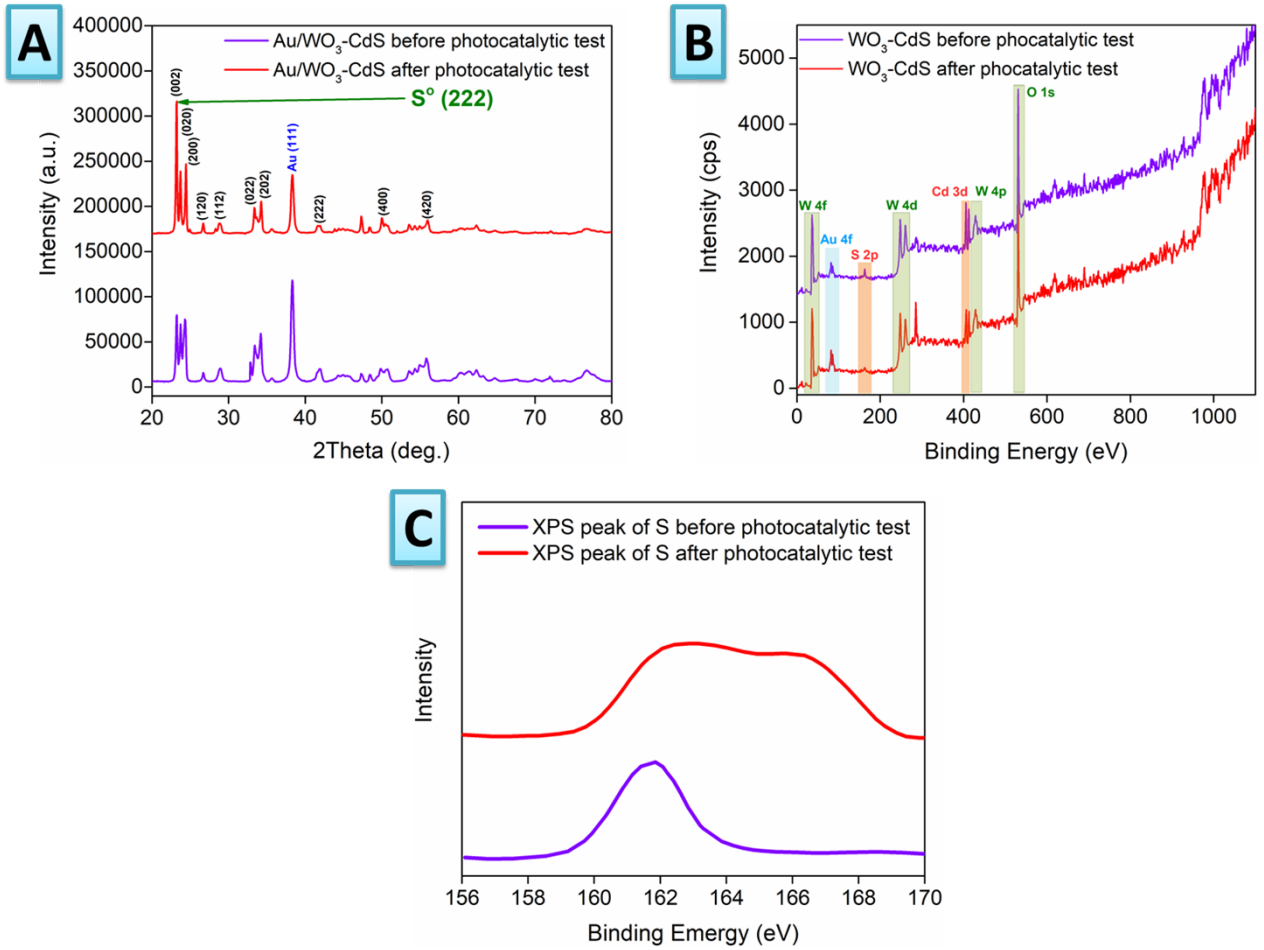


**Fig. S15** XRD (A) and XPS (B) results of $WO_3$-CdS samples before and after photocatalytic stability test; (C) – deconvolution of characteristic sulphur XPS peak.

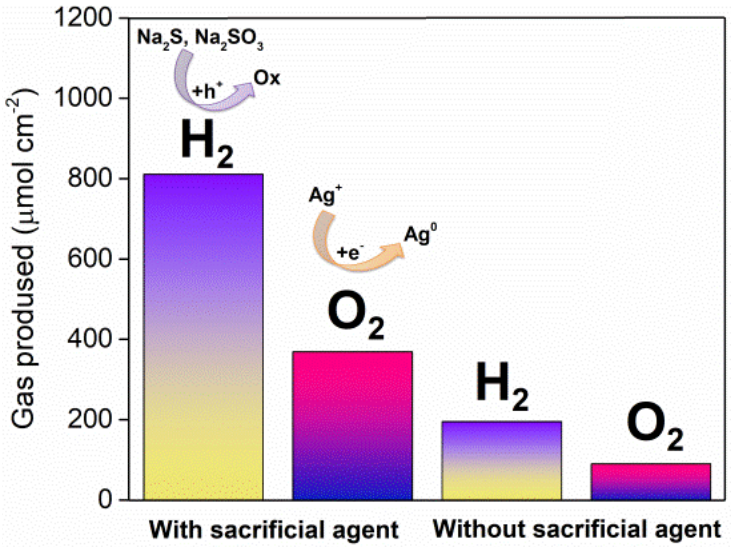


**Fig. S16** Amount of oxygen and hydrogen produced in the presence of sacrificial agents (0,35M $Na_2S$ and 0,25M $Na_2SO_3$ for hydrogen evolution; 0,1M $AgNO_3$ for oxygen evolution cases) in comparison with pure water, i.e. without sacrificial agent

## References

[S1] J. Fu, Q. Xu, J. Low, C. Jiang and J. Yu, *Appl. Catal. B.*, 2019, **243**, 556–565.

[S2] G. Socrates, *Infrared and Raman Characteristic Group Frequencies: Tables and Charts*, John Wiley & Sons, 2004

[S3] Y. Kalachyova, D. Mares, V. Jerabek, K. Zaruba, P. Ulbrich, L. Lapcak, V. Svorcik and O. Lyutakov, *J. Phys. Chem. C*, 2016, **120**, 10569–10577.